Int. J. Non-Linear Mechanics, Vol. 20, No. 4, pp. 325–338, 1985
Printed in Great Britain.

0020–7462/85 $03.00 + .00
Pergamon Press Ltd.

DYNAMICS OF A SYSTEM EXHIBITING THE GLOBAL BIFURCATION OF A LIMIT CYCLE AT INFINITY

W. L. KEITH and R. H. RAND

Department of Theoretical and Applied Mechanics, Thurston Hall, Cornell University, Ithaca, NY 14853, U.S.A.

(*Received* 26 *July* 1984; *received for publication* 7 *March* 1985)

Abstract—This paper concerns the dynamics of a class of non-linear oscillators of the form:

$$x'' + x - \varepsilon x'(1 - ax^2 - bx'^2) = 0.$$

The non-linear term contains two parameters a and b which may be varied to give the Rayleigh and Van der Pol differential equations as special cases.

The existence and approximation of limit cycles in this system are investigated using the Poincare–Bendixson theorem and the Lindstedt perturbation method. Analysis of the system at infinity is used to study the global bifurcation through which the limit cycle is created from four saddle–saddle connections between equilibrium points at infinity. Center manifold theory is used to determine the stability of the equilibrium points at infinity. Numerical integration is used to verify the analytical results.

It is shown that an arbitrarily small perturbation to the damping term of the Rayleigh equation results in points close to the stable limit cycle escaping to infinity.

INTRODUCTION

We consider the non-linear differential equation:

$$x'' + x - \varepsilon x'(1 - ax^2 - bx'^2) = 0 \quad \text{or} \quad \begin{cases} x' = y \\ y' = -x + \varepsilon y(1 - ax^2 - by^2) \end{cases} \tag{1}$$

where $\varepsilon > 0$ (but not necessarily small), and where the natural frequency of the $\varepsilon = 0$ equation has been taken as unity.

When $a = 0$ and $b = 1/3$ we have Rayleigh's equation ([1], p. 81):

$$x'' + x - \varepsilon x'(1 - x'^2/3) = 0 \tag{2}$$

and when $a = 1$ and $b = 0$ we have Van der Pol's equation [2]:

$$x'' + x - \varepsilon x'(1 - x^2) = 0. \tag{3}$$

Note that (3) may be obtained from (2) by differentiating (2) with respect to time t and taking the variable x in (3) to be x' in (2). Both (2) and (3) are known to exhibit stable limit cycles for all values of $\varepsilon > 0$ ([3], p. 3).

Equation (1) possesses exactly one equilibrium point in the finite phase plane located at the origin for all a, b and ε. In view of the assumption that $\varepsilon > 0$, it is an unstable node ($\varepsilon > 2$) or unstable focus ($0 < \varepsilon < 2$).

Note that since equation (1) is invariant under replacement of (x, y) by $(-x, -y)$, the flow (1) is point-symmetric about the origin (i.e. it is invariant under a rotation of π radians).

It turns out that equation (1) exhibits a limit cycle in the x, y phase plane for some values of the parameters. We shall be interested in determining regions in the a,b parameter plane for which a limit cycle exists. We will investigate this question by applying a variety of techniques, including examining the system at infinity (i.e. for large x, y). Information gained from the behavior of the system at infinity will be shown to explain the global bifurcations which lead to the creation of the limit cycle. The symbolic manipulation system MACSYMA [4] has been used extensively in this work.

LIMIT CYCLES

Equation (1) exhibits a stable limit cycle for all positive values of a, b and ε. This may be proved by using the Poincare–Bendixson theorem ([5], p. 84), which states that a stable limit cycle exists in any annular region R which (i) contains no equilibria, and (ii) has boundary curves $C1$ and $C2$ such that the flow of (1) enters the region R at all points on $C1$ and $C2$.

We choose R to be bounded by the circles (Fig. 1):

$$C1: x^2 + y^2 = r_1^2 < 1/a \tag{4}$$

$$C2: x^2 + y^2 = r_2^2 > 1/b. \tag{5}$$

On the inner circle, $C1$, the unit normal pointing into R is the radially outward vector $(x/r_1, y/r_1)$, and the component of the vector field of (1) in the radial direction is given by the dot product

$$\frac{x}{r_1}y + \frac{y}{r_1}[-x + \varepsilon y(1 - ax^2 - by^2)] = \frac{\varepsilon y^2}{r_1}(1 - ar_1^2 + (a - b)y^2) \tag{6}$$

which is nonnegative in view of the assumptions $a \geq b, r_1^2 < 1/a$. Therefore at no point on $C1$ does the vector field of (1) point out of R. A similar statement holds for $C2$.

Note that the Poincare–Bendixson theorem offers only sufficient conditions for the existence of a limit cycle. Thus, although we have proven that (1) possesses at least one stable limit cycle for all positive a, b and ε (Fig. 2), we may not conclude that limit cycles do not exist for other values of the parameters. We will now utilize the Lindstedt perturbation method to find those values of a, b for which a limit cycle exists in the small ε limit.

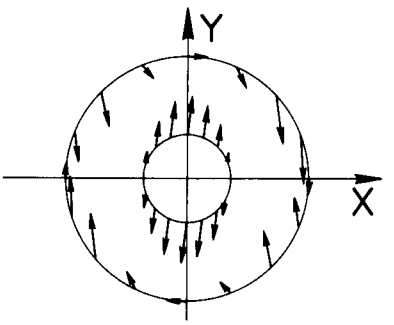

Fig. 1. The vector field is shown on the circles C_1 and C_2 given by $r_1^2 = 1/a$ and $r_2^2 = 1/b$, respectively. Here $a = 2$, $b = 1$, and $\varepsilon = 10$. A limit cycle exists within the annular region. The case $a < b$ may be handled analogously.

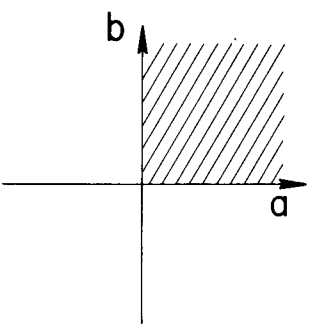

Fig. 2. The region in a, b parameter space in which a limit cycle may be proven to exist by the Poincare–Bendixson theorem.

LINDSTEDT'S METHOD

In order to apply Lindstedt's method [6] to (1) we stretch time (thereby allowing the frequency of the oscillator to differ from its $\varepsilon = 0$ value of unity):

$$\tau = (1 + \varepsilon\omega_1 + \varepsilon^2\omega_2^2 + \cdots)t \tag{7}$$

and expand x in a power series in ε.

$$x = x_0 + \varepsilon x_1 + \varepsilon^2 x_2^2 + \cdots. \tag{8}$$

We substitute (7) and (8) into (1), collect terms, and equate to zero the coefficient of ε^n. This generates a sequence of differential equations on the $x_i(\tau)$. The function $x_0(\tau)$ satisfies

$$x_0'' + x_0 = 0 \tag{9}$$

where primes now represent differentiation with respect to τ. Since (1) is autonomous, we may without loss of generality choose the initial condition

$$x_0'(0) = 0 \tag{10}$$

giving

$$x_0 = A_1 \cos(\tau). \tag{11}$$

The function $x_1(\tau)$ satisfies

$$x_1'' + x_1 = -2\omega_1 x_0'' + x_0' - a x_0' x_0^2 - b x_0'^3. \tag{12}$$

Substituting (11) into (12) and eliminating secular terms gives

$$\omega_1 = 0 \text{ and } A_1 = 2/\sqrt{(3b + a)}. \tag{13}$$

The approximate amplitude A_1 of the limit cycle will be real only if

$$3b + a > 0. \tag{14}$$

This approximate analysis suggests (but does not prove) that a limit cycle exists for small ε in the region of a, b parameter space defined by (14). See Fig. 3.

NUMERICAL INTEGRATION

Comparison of Figs 2 and 3 suggests that for a given value of ε, equation (1) exhibits a limit cycle for all parameter values a and b in a region of the a, b plane which includes the first quadrant. For small ε this region is the half plane $(3b + a) > 0$ (Fig. 3). As ε is increased, it

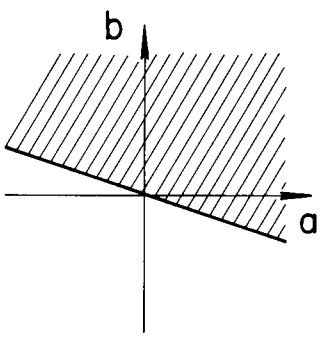

Fig. 3. The region in a, b parameter space in which the presence of a limit cycle is indicated by the Lindstedt perturbation method. The boundary is given by $b = -a/3$.

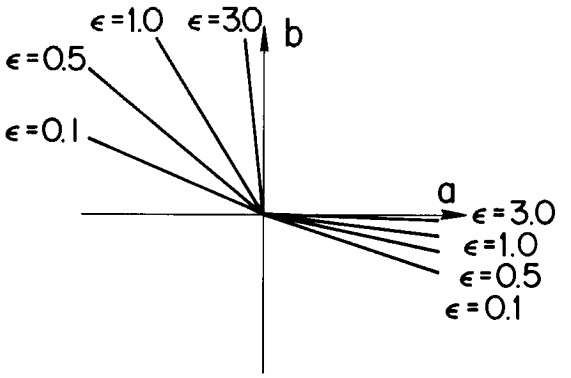

Fig. 4. The bounding curves in a, b parameter space (for fixed ε), above which a limit cycle exists. These results are obtained by numerical integration.

turns out that the corresponding region becomes smaller, until, in the limit as ε approaches infinity, the limit cycle exists only in the first quadrant in the a, b plane (Fig. 2). This statement is illustrated in Fig. 4 which is based on the following numerical investigation.

We numerically integrated equation (1) using a fourth order Runge–Kutta scheme with step size 0.1. For given ε and b, we varied a and integrated for 1000 time steps. By examining the resulting phase portraits, we were able to estimate the value of a at which the limit cycle first appeared. Note that the bifurcation curves in Fig. 4 are approximately straight lines.

Regarding the nature of the bifurcation which gave rise to the limit cycle, the phase portraits obtained from numerical integration showed that as one crossed a bifurcation curve in Fig. 4 (for fixed ε), the limit cycle was evidently created with infinite amplitude, i.e. it bifurcated in from infinity. This result is in agreement with the expression (13) for the limit cycle amplitude A_1 obtained by Lindstedt's method: A_1 blows up as $3b + a$ changes sign.

In order to better understand the nature of this bifurcation, we shall examine the behavior of the system (1) at infinity.

BEHAVIOR AT INFINITY

In order to investigate the behavior of the system (1) for large x and y, we use Poincare's scheme of considering the associated flow on the projective plane ([5], p. 91, [7], p. 10). This consists of identifying a point in the plane with a point on a unit hemisphere sitting at the origin, via a projection through the center of the hemisphere (Fig. 5). Diametrically opposite points on the equator of the hemisphere correspond, in pairs, to points at infinity on the plane.

This scheme can be effected by a transformation from x, y to u, z coordinates ([5], p. 92):

$$u = x/y, \qquad z = 1/y. \tag{15}$$

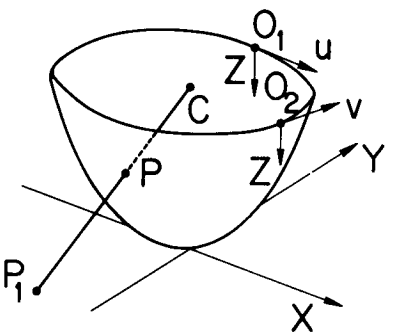

Fig. 5. The projective plane ($= \mathbb{R}^2$ plus a line at infinity) identified with the points on a unit hemisphere. A ray projected from the hemisphere's center C associates a point P on the hemisphere with a point P_1 on the plane. Points at infinity correspond to the equator of the hemisphere. Points 0_1 and 0_2 are the respective origins of the coordinate transformations (15) and (16) and lie at the ends of the y and x axes.

Here $z = 0$ corresponds to the equator of the hemisphere, and u measures the angular position around the equator (Fig. 5).

Before using (15), we note that it is not valid in the neighborhood of $y = 0$. To study points which lie at the "ends" of the x-axis, we may use the alternate transformation (Fig. 5):

$$v = y/x, \qquad z = 1/x. \tag{16}$$

Under the transformation (15), equation (1) becomes:

$$\begin{aligned} z' &= uz^3 - \varepsilon z(z^2 - au^2 - b) \\ u' &= z^2(1 + u^2) - \varepsilon u(z^2 - au^2 - b) \end{aligned} \tag{17}$$

where primes represent differentiation with respect to a stretched time τ defined by $dt/d\tau = z^2$.

Note that $z = 0$ identically satisfies (17), i.e. the equator on the hemisphere (or the set of points at infinity in the plane) is an invariant manifold. The flow on the equator $z = 0$ is given by:

$$u' = \varepsilon u(au^2 + b), \qquad z = 0 \tag{18}$$

which leads to the following equilibrium points at infinity:

$$u = 0, \qquad z = 0 \tag{19}$$

$$u = \pm\sqrt{(-b/a)}, \qquad z = 0 \quad \text{when} \quad -b/a > 0. \tag{20}$$

Note that each of these equilibria at infinity in fact represents two points on the equator, since diametrically opposite points are identified.

To check the points at the ends of the x-axis, we transform (1) using (16) to obtain:

$$\begin{aligned} z' &= -vz^3 \\ v' &= -\varepsilon v(a + bv^2) + z^2(\varepsilon v - v^2 - 1) \end{aligned} \tag{21}$$

where again primes represent differentiation with respect to the stretched time τ, where $dt/d\tau = z^2$.

From (21) we see that another equilibrium at infinity is given by:

$$v = 0, \qquad z = 0. \tag{22}$$

We may summarize these results as follows: In the second and fourth quadrants of the a, b parameter plane, in which $-b/a > 0$, there are four distinct diametrically opposite pairs of equilibrium points at infinity given by (19), (20) and (22). In the first and third quadrants only two diametrically opposite pairs of equilibria exist, (19) and (22). As one crosses the a or b axes, the equilibria (20) coalesce with the equilibria (19) or (22), respectively, via pitchfork bifurcations, to be discussed in more detail later in this paper.

In order to investigate the stability of these equilibria, we linearize in their neighborhoods. We begin with equation (19), and linearize (17), about $u = z = 0$:

$$z' = \varepsilon bz, \qquad u' = \varepsilon bu \tag{23}$$

Thus for $b > 0$, (19) is an unstable node, while for $b < 0$, (19) is a stable node (we assume $\varepsilon > 0$ throughout). See Fig. 6 where we are looking down into the hemisphere from above the x, y plane.

Next let us consider equation (22). Linearization of (21) about $v = z = 0$ gives:

$$z' = 0, \qquad v' = -\varepsilon av. \tag{24}$$

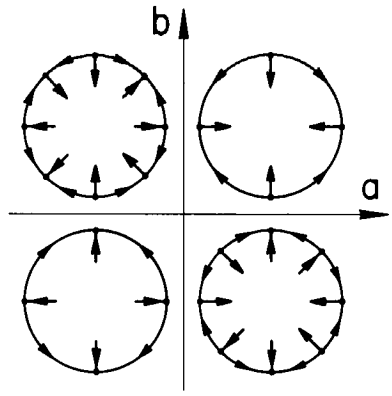

Fig. 6. The equilibrium points at infinity (lying on the equator of the unit hemisphere in Fig. 5) and their stability, corresponding to the four regions in a, b parameter space. Diametrically opposite points on the equator of the hemisphere represent the same points at infinity in the x, y plane.

In the case that $a < 0$, this equilibrium is unstable. For $a > 0$, however, this linear system has one negative and one zero eigenvalue, and thus its stability cannot be determined from (24). This situation is the critical case of Liapunov ([5], p. 150).

We shall determine the stability of the equilibrium (22) in the case $a > 0$ by the use of center manifold theory [8]. For this problem, the center manifold theorem states that there is a curve $v = f(z)$ which is tangent to the z-axis at the origin $v = z = 0$ (being the eigendirection corresponding to the zero eigenvalue), and to which all neighboring solutions tend asymptotically as τ goes to infinity. This curve, called the center manifold, is, moreover, invariant under the full non-linear flow (21). The center manifold theorem tells us that the stability of the equilibrium (22) is determined by the flow on the center manifold.

In order to formally approximate the center manifold, we expand $v = f(z)$ in a power series:

$$v = f(z) = a_2 z^2 + a_3 z^3 + \cdots \tag{25}$$

where we have omitted the constant and linear terms in (25) in order for $f(z)$ to be tangent to the z-axis at $z = 0$. We may obtain the coefficients a_i as follows:

(i) Differentiate (25) with respect to τ;
(ii) Substitute the differential equations (21) into (i);
(iii) Substitute (25) into (ii) so that the only variable appearing is z;
(iv) Collect terms and require the coefficient of z^n to vanish.

It will turn out that for the stability determination, we will only need the leading term in (25). In fact, the algebra involved in the computation of additional terms rapidly grows burdensome, and the computer algebra system MACSYMA has proved extremely useful in the computation of center manifolds [4, 12].

Following the above steps (i)–(iv), we find this approximate expression for the center manifold:

$$v = -\frac{z^2}{\varepsilon a} + O(z^3). \tag{26}$$

Substituting (26) into the first of (21) gives the following approximation for the flow on the center manifold:

$$z' = \frac{z^5}{\varepsilon a} + O(z^6) \tag{27}$$

from which it follows that the flow on the center manifold is unstable for $a > 0$ and stable for $a < 0$.

In summary, the equilibrium (22) is a saddle for $a \neq 0$. See Fig. 6.

We now come to the pair of equilibria (20). Our first step is to translate coordinates from u, z to w, z so that $w = z = 0$ corresponds to the equilibrium. We set

$$w = u - \sqrt{-b/a} \tag{28}$$

where we have taken the positive square root. Substitution of (28) into (17) gives a pair of differential equations on z and w, which we omit here. Linearization about $z = w = 0$ reveals that the eigenvalues are zero and $-2\varepsilon b$. We once again look for a center manifold tangent to the z-axis, and proceeding as before, we find this approximation for the center manifold:

$$w = \frac{1 - b/a - \varepsilon\sqrt{(-b/a)}}{2\varepsilon b} z^2 + O(z^3). \tag{29}$$

Substitution of (29) into the z' equation gives the following flow on the center manifold:

$$z' = -\sqrt{(-a/b)}z^3 + O(z^4) \tag{30}$$

which is stable. Thus the non-zero eigenvalue, $-2\varepsilon b$, determines the stability. This equilibrium is a saddle for $a > 0$, $b < 0$, and a stable sink for $a < 0$, $b > 0$. See Fig. 6.

The case of the negative square root equilibrium in (20) is handled similarly. This time we set

$$w = u + \sqrt{(-b/a)}. \tag{31}$$

As before, we substitute (31) into (17) and linearize about $z = w = 0$ again giving the eigenvalues zero and -2ε. We once again look for a center manifold tangent to the z-axis, and find this approximation for the center manifold:

$$w = \frac{1 - b/a + \varepsilon\sqrt{(-b/a)}}{2\varepsilon b} z^2 + O(z^3). \tag{32}$$

Substitution of (32) into the z' equation gives the following flow on the center manifold:

$$z' = +\sqrt{(-a/b)}z^3 + O(z^4) \tag{33}$$

which is unstable. Thus the equilibrium is a saddle for $a < 0$, $b > 0$, and an unstable source for $a > 0$, $b < 0$. See Fig. 6.

This completes the description of how we obtained the information to sketch Fig. 6.

GLOBAL BIFURCATION OF THE LIMIT CYCLE

We return now to results obtained by numerical integration. For a given value of ε, there are 6 distinct regions in the a, b plane, each with its own characteristic phase portrait. For each of these regions, we display in Fig. 7 a sketch of the flow on the hemisphere (as seen from above). Note that each phase portrait is point-symmetric about the origin. Also, there are points which are close to the stable limit cycle, but do not approach it, and points which come from and or go to equilibria at infinity.

In region I, all trajectories (except the origin) approach the stable limit cycle as t approaches positive infinity. In region II, trajectories within the shaded regions do not approach the limit cycle. The shaded regions contain points which come from and go to equilibria at infinity. In region III, the limit cycle no longer exists, but shaded regions are still present. Here, all trajectories (except the origin) go to equilibria at infinity. This last statement also holds for region IV, in which neither the limit cycle nor the shaded regions exist. Regions V and VI are similar to regions III and II, respectively.

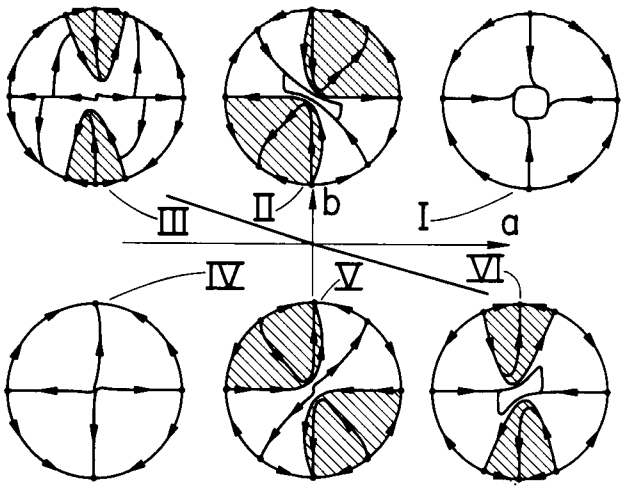

Fig. 7. The global phase portraits corresponding to the six regions in parameter space, obtained from numerical integration and stability analysis of the fixed points at infinity. Points lying in the shaded regions come from and go to equilibria at infinity. Here $\varepsilon = 0.1$.

We are interested in characterizing the bifurcation which gives rise to the limit cycle as one goes from region III to II, or from region V to VI. We consider this bifurcation in detail in Fig. 8 by displaying schematic phase portraits for points in the a, b plane which are:

(i) in region III (no limit cycle exists);
(ii) on the boundary between regions II and III (a closed loop consisting of four saddle–saddle connections between points at infinity exists);
(iii) in region II (a limit cycle exists).

In Fig. 8(i), saddle–sink and source–sink connections exist in the finite portion of the phase space between points A and C, and between B and C, respectively. In addition, the line at infinity (the equator of the hemisphere) connects points A to B, B to C, C to D, etc. At the bifurcation, Fig. 8(ii), the saddle–sink connection between A and C is broken, being replaced by a saddle–saddle connection between A and D. In Fig. 8(iii), the latter connection is broken, and replaced by a source–saddle connection between B and D. The closed loop of saddle–saddle connections A–D–C'–D'–A in Fig. 8(ii) forms the limit cycle in Fig. 8(iii). This homoclinic bifurcation involves four saddle separatrices. For the more general case in which each of the fixed points forming such a loop are hyperbolic, the bifurcation of a limit cycle may be proven using the Theorem of Reyn [9]. For our case however, none of the four fixed points are hyperbolic, and this theorem does not apply.

This bifurcation may be characterized by the existence of a saddle–saddle connection between points A and D. We shall use this fact in order to obtain an approximate analytical relationship between the parameters a, b and ε which holds at the bifurcation occurring between regions II and III (cf. Fig. 4, where such a relationship was obtained numerically).

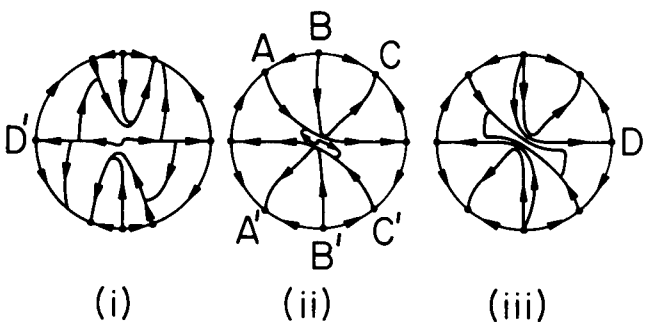

Fig. 8. The bifurcation of the limit cycle occurring in passing from region III to region II in a, b parameter space. Here $a = -7.5$, $\varepsilon = 0.1$, and (i) $b < b_{crit}$, (ii) $b = b_{crit}$, (iii) $b > b_{crit}$.

The saddle–saddle connection between points A and D, called S in the following, behaves like the center manifold (32) near point A, and like (26) near point D. In x, y coordinates, equation (32) can be written:

$$y = -\sqrt{-a/b}\,x - \frac{1 - b/a + \varepsilon\sqrt{-b/a}}{2\varepsilon b x} + \cdots . \tag{34}$$

Similarly, equation (26) can be written:

$$y = \frac{-1}{a\varepsilon x} + \cdots . \tag{35}$$

The expressions (34) and (35) are good approximations for the saddle–saddle connection S as x goes to negative and positive infinity, respectively. In the neighborhood of $x = 0$, a comparable expression may be obtained by expanding equation (1) in a Taylor series ([4], p. 42):

$$y = y_0 + \varepsilon(1 - by_0^2)x + \cdots \tag{36}$$

where y_0 is the value of S when $x = 0$ (y_0 is to be found). Fig. 9 displays equations (34)–(36).

In order to approximate S, we patch equations (34)–(36) as follows: We require equations (34) and (36) to have equal slopes at their point of intersection, defined by $x = x_L < 0$. Similarly we require equations (35) and (36) to have equal slopes at their point of intersection, $x = x_R > 0$. This results in four non-linear algebraic equations, from which x_L, x_R and y_0 may be eliminated, leaving the desired relationship between the parameters a, b and ε. Using MACSYMA, we find:

$$-(4b + a)\sqrt{\left(\frac{-a}{b}\right)} - a\varepsilon + \frac{2b\varepsilon}{1 + \dfrac{-b}{a} + \varepsilon\sqrt{\left(\dfrac{-b}{a}\right)}} = 0 \tag{37}$$

(note $a < 0$, $b > 0$ in the above).

Equation (37) is the approximate condition for the bifurcation occurring between regions II and III. It gives results which are qualitatively the same as those found numerically in Fig. 4. See Fig. 10 where equation (37) is compared with the numerically obtained results. Presumably greater accuracy could be obtained by including additional terms in the series expansions (34)–(36). We found, however, that the inclusion of additional terms rendered the problem intractable on MACSYMA.

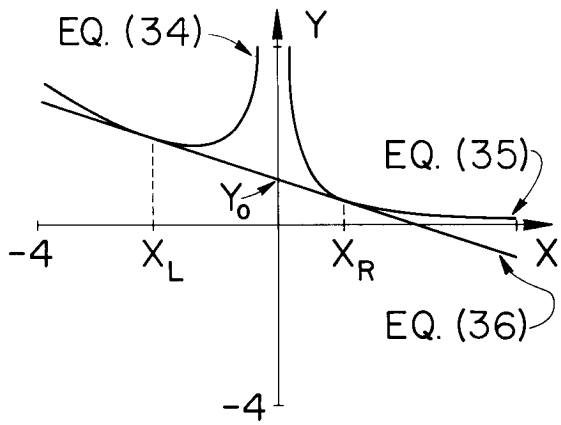

Fig. 9. The approximation of the A–D saddle–saddle separatrix is obtained by patching the center manifold from points A and D to the Taylor series approximation near the origin. Here $a = -0.5$, $b = 1$, $\varepsilon = 3$, $Y_0 = 1.07$, $X_L = -2.1$, and $X_R = 1.2$.

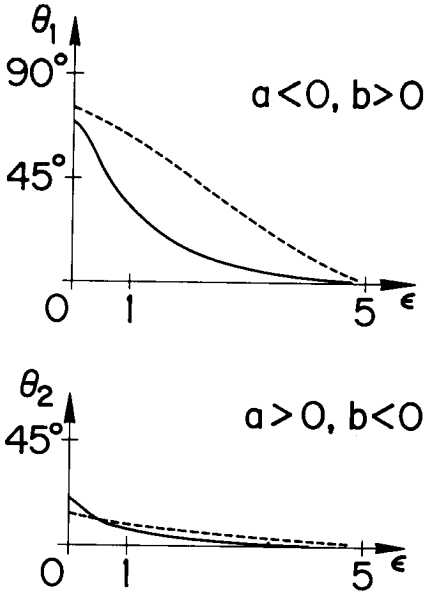

Fig. 10. The dotted and solid lines denote the patching and numerical results, respectively, for the transition curves in a, b parameter space. θ_1 is measured counterclockwise from the b axis to the curves in the second quadrant, and θ_2 is measured clockwise from the a axis to the curves in the fourth quadrant. The upper dotted line is based on equation (37) and the lower dotted line on equation (38).

A similar computation may be performed for the bifurcation occurring between regions V and VI. The resulting relationship between a, b and ε for the bifurcation is found to be:

$$+(4b+a)\sqrt{\left(\frac{-a}{b}\right)} - a\varepsilon + \frac{2b\varepsilon}{1+\dfrac{-b}{a} - \varepsilon\sqrt{\left(\dfrac{-b}{a}\right)}} = 0 \tag{38}$$

(note $a > 0$, $b < 0$ in the above).

Equation (38) is compared with numerically obtained results in Fig. 10.

VAN DER POL'S AND RAYLEIGH'S EQUATIONS

As mentioned previously, Van der Pol's and Rayleigh's equations are special cases of the class of systems (1). From the point of view of this embedding, these well known equations are very singular, and lie along the boundaries between regions I and VI, and regions I and II, respectively. The pitchfork bifurcation of equilibria at infinity [see equation (20)] has its point of origin along these boundaries, and hence Van der Pol's and Rayleigh's equations possess particularly singular equilibria at infinity.

Consider, e.g. Van der Pol's equation (3) for which $a = 1$ and $b = 0$. For these parameter values, equation (17) becomes:

$$\begin{aligned} z' &= uz^3 - \varepsilon z(z^2 - u^2) \\ u' &= z^2(1+u^2) - \varepsilon u(z^2 - u^2). \end{aligned} \tag{39}$$

On the invariant manifold $z = 0$, we obtain the flow:

$$u' = \varepsilon u^3.$$

In terms of the flow on the equator of the hemisphere, $u = 0$ is unstable for $\varepsilon > 0$.

Note that (39) has no linear terms about $u = z = 0$. However, if we set $\xi = z^2$, equations (39) may be written:

$$\begin{aligned} u' &= \xi - \varepsilon u\xi + O(3) \\ \xi' &= -2\varepsilon\xi^2 + O(3). \end{aligned} \tag{40}$$

Equations (40) have the linear part

$$\begin{bmatrix} 0 & 1 \\ 0 & 0 \end{bmatrix}. \tag{41}$$

The presence of a double zero eigenvalue in (41) means that (40) has a two dimensional center manifold. Systems of this form have been studied by Takens [10]. Guckenheimer and Holmes have summarized Taken's work, and we follow them here. The system

$$\begin{bmatrix} X' \\ Y' \end{bmatrix} = \begin{bmatrix} 0 & 1 \\ 0 & 0 \end{bmatrix} \begin{bmatrix} X \\ Y \end{bmatrix} + O(2) \tag{42}$$

can always be reduced by a near-identity transformation to the normal form:

$$\begin{bmatrix} X_1' \\ Y_1' \end{bmatrix} = \begin{bmatrix} 0 & 1 \\ 0 & 0 \end{bmatrix} \begin{bmatrix} X_1 \\ Y_1 \end{bmatrix} + \begin{bmatrix} 0 \\ AX_1^2 + BX_1Y_1 \end{bmatrix} + O(3) \tag{43}$$

where X_1 and Y_1 are the transformed variables, and where A and B are constants. Guckenheimer and Holmes [11] state that if the coefficient $A \neq 0$, then (43) is "determined", i.e. the topological nature of the local phase portrait is not influenced by $O(3)$ terms.

In the case of equation (40), however, we can set

$$\begin{aligned} u &= X_1 - 3\varepsilon X_1^2/2 \\ \xi &= Y_1 - 2\varepsilon X_1 Y_1 \end{aligned} \tag{44}$$

which turns out to transform (40) to the form of (43) with $A = 0$ and $B = 0$. This unfortunately means that (40) is not determined by its quadratic terms, and therefore existing normal form theory is of no help to us here.

We may nevertheless numerically integrate equations (39). The result is displayed in Fig. 11.

Van der Pol's equation also has another equilibrium at infinity. It is governed by equations (21), which in this case become:

$$\begin{aligned} z' &= -vz^3 \\ v' &= -\varepsilon v + z^2(\varepsilon v - v^2 - 1). \end{aligned} \tag{45}$$

The equilibrium $v = z = 0$ has eigenvalues zero and $-\varepsilon$. There is a center manifold tangent to the z-axis of the form:

$$v = -z^2/\varepsilon + O(3) \tag{46}$$

Substitution of (46) into the z' equation of (45) gives:

$$z' = z^5/\varepsilon + \cdots \tag{47}$$

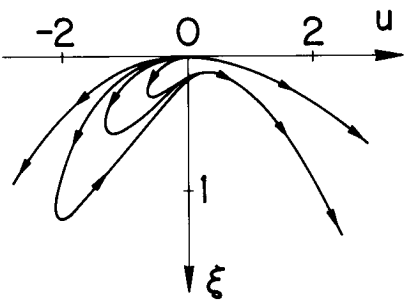

Fig. 11. The trajectories near the nonhyperbolic fixed point B at infinity for the Van der Pol equation. Here $\varepsilon = 1.0$. These results are obtained by numerical integration of equations (39).

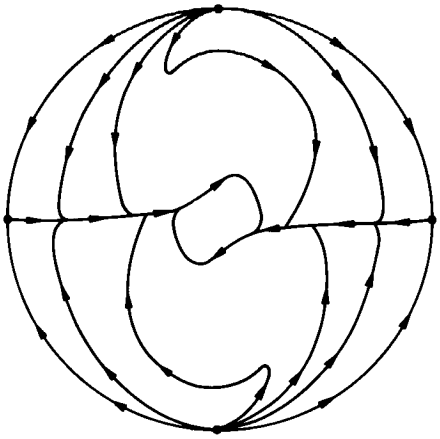

Fig. 12. The global phase portrait for the Van der Pol equation. Here $\varepsilon = 1.0$.

which means that the flow on the center manifold is unstable for $\varepsilon > 0$, and the equilibrium is a saddle. These results for the Van der Pol equation are displayed on the hemisphere in Fig. 12.

Now we consider Rayleigh's equation (2) for which $a = 0$ and $b = 1/3$. For these parameter values, the equilibrium at $u = z = 0$ of equation (17) has already been shown in equation (23) to be an unstable node. In contrast to both equilibria at infinity in the Van der Pol equation, this equilibrium is hyperbolic, i.e. its stability is completely determined by the linear terms in its Taylor series expansion about $u = z = 0$; no center manifolds are involved here.

The other equilibrium at infinity in Rayleigh's equation, at $v = z = 0$, is quite singular, however. In this case equations (21) become:

$$\begin{aligned} z' &= -vz^3 \\ v' &= -\varepsilon v^3/3 + z^2(\varepsilon v - v^2 - 1). \end{aligned} \tag{48}$$

Although (48) has no linear terms about $v = z = 0$, we may set $\xi = -z^2$, where upon (48) becomes

$$\begin{aligned} v' &= \xi - \varepsilon v\xi + O(3) \\ \xi' &= \quad 0 \quad + O(3) \end{aligned} \tag{49}$$

which is of the form of (42). By using the near-identity transformation

$$\begin{aligned} v &= X_1 - \varepsilon X_1^2/2 \\ \xi &= Y_1 \end{aligned} \tag{50}$$

equation (49) can be put in the form of (43) with $A = B = 0$. As in the case of the $u = z = 0$ equilibrium in Van der Pol's equation, this means that the flow in the neighborhood of this equilibrium is not determined by its quadratic terms, and the existing normal form theory is inapplicable here [12].

In order to gain a better understanding of this equilibrium, we numerically integrated equations (48). The results are displayed in Figs 13 and 14.

Figure 14 shows that the limit cycle associated with the Rayleigh equation is globally attracting. An imbedding for the Rayleigh equation is given by equation (1) with $b = 1/3$, for varying a. As a goes from $-\delta$ to $+\delta$ (where $|\delta| \ll 1$), the nongeneric pitchfork bifurcation shown in Fig. 15(ii) occurs at point D. The stable and unstable fixed points C and C', respectively, coalesce with the unstable fixed point D and disappear. Figure 15(i) shows a portion of the global phase portrait for $a = -0.1$. The analogous portrait for $a = 0$ is contained in Fig. 14. Throughout this bifurcation, the stable limit cycle persists, and point D remains an unstable fixed point. However, the large shaded region shown in Fig. 15(i) (in

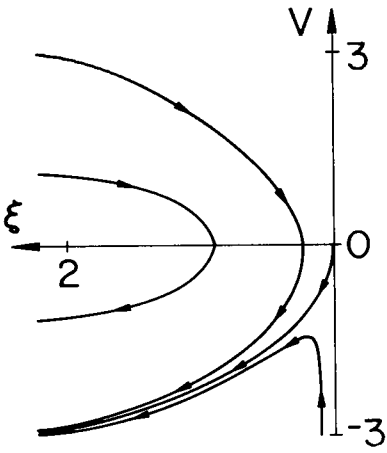

Fig. 13. The trajectories near the nonhyperbolic fixed point D for the Rayleigh equation. Here $\varepsilon = 1.0$. These results are obtained from numerical integration of equations (48).

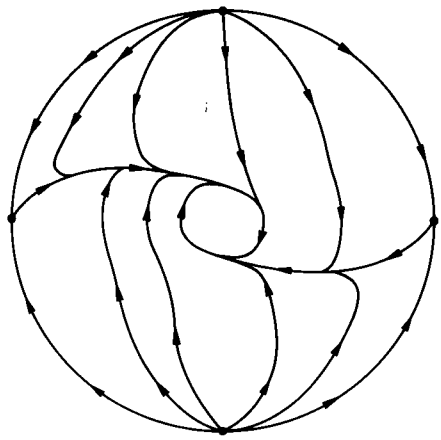

Fig. 14. The global phase portrait for the Rayleigh equation. Here $\varepsilon = 1.0$.

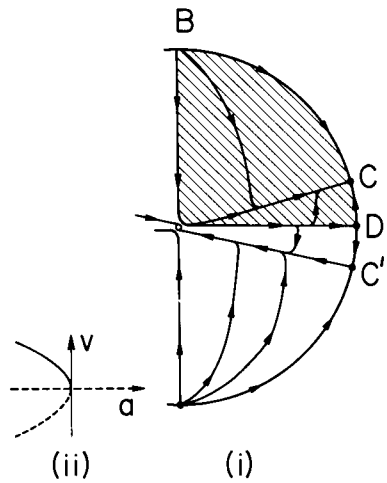

Fig. 15. (i) The global phase portrait for $x > 0$ in the Rayleigh equation. Points in the shaded region come from and go to equilibria at infinity. Other points approach the stable limit cycle near the origin. Here $a = -0.1$, $b = 1$, and $\varepsilon = 0.1$. (ii) The pitchfork bifurcation diagram for the nonhyperbolic fixed point D at infinity. Dashed and solid lines denote unstable and stable fixed points, respectively. Note that while the equilibrium point D corresponding to the handle of the pitchfork does change stability at $a = 0$ when restricted to the flow at infinity (i.e. on the equator of the hemisphere), it remains unstable for all values of a when considered as part of the flow on the two dimensional hemisphere.

which all trajectories approach infinity) disappears at the bifurcation, and the limit cycle becomes globally attracting. Therefore, the addition of the arbitrarily small term $-\delta x^2$ to the coefficient $1 - \dot{x}^2/3$ of the $\varepsilon\dot{x}$ damping term in the Rayleigh equation, although not affecting the existence of the stable limit cycle, does result in the escape to infinity of virtually all of the points lying in the first and third quadrants in the x, y phase plane. The nature of the pitchfork bifurcation associated with the Van der Pol equation is similar, and occurs at point B.

Note that while the Van der Pol equation may be trivially obtained from the Rayleigh equation [see comment after equation (3)], their respective behavior at infinity is quite different.

Acknowledgements—The authors wish to thank Professor Philip Holmes for helpful suggestions. This work was supported by Air Force Grant No. AFOSR-84-0051.

REFERENCES

1. J. W. S. Rayleigh, *Theory of Sound*, Vol. 1, Dover, New York (1945).
2. B. Van der Pol, Relaxation oscillations. *Phil. Mag.* **7**, 978–992 (1926).
3. A. H. Nayfeh and D. T. Mook, *Non-linear Oscillations*. John Wiley, New York (1979).
4. R. H. Rand, *Computer Algebra in Applied Mathematics: An Introduction to MACSYMA*. Research Notes in Mathematics, Pitman, Boston, MA (1984).
5. M. Minorsky, *Non-linear Oscillations*. Kreiger, New York (1974).
6. J. J. Stoker, *Non-linear Vibrations*, Wiley Interscience, New York (1950).
7. H. Seifert and W. Threlfall, *A Textbook of Topology*. Academic Press, New York (1980).
8. J. Carr, *Applications of Centre Manifold Theory*. Springer, New York (1981).
9. J. W. Reyn, A stability criterion for separatrix polygons in the phase plane. *Nieuw Archief Voor Wiskunde* **27**(3), 238–254 (1979).
10. F. Takens, Singularities of vector fields. *Publ. Math. IHES* **43**, 47–100 (1974).
11. J. Guckenheimer and P. J. Holmes, *Non-linear Oscillations, Dynamical Systems and Bifurcations of Vector Fields*. Springer, New York (1983).
12. R. H. Rand and W. L. Keith, Normal form and center manifold calculations on MACSYMA. In *Applications of Computer Algebra* (Edited by R. Pavelle). Kluwer, Boston (1985).